International Forum on Aeroelasticity and Structural Dynamics
IFASD 2017
25-28 June 2017 Como, Italy

EFFECT OF ANGLE OF ATTACK, GAS COMPOSITION AND REYNOLDS NUMBER ON FLUTTER BOUNDARY OF BENCHMARK SUPER-CRITICAL WING

Jan Navrátil[1], Adam Jirásek[2], Peter Hamlington[2], Lt. Col. Andrew Lofthouse[3]

[1]Institute of Aerospace Engineering
Brno University of Technology, VUT
Technická 2896/2, 616 69 Brno, Czech Republic
navratil@fme.vutbr.cz

[2]Mechanical Engineering, Colorado University, Boulder, USA
[3]Department of Aeronautics
US Air Force Academy, USAFA, USA

Keywords: flutter, transonic, computational, fluid, dynamics, BSCW, AePW, aeroelasticity

Abstract: This paper presents results of the second Aeroelastic Prediction Workshop which uses the Benchmark Super-Critical Wing, BSCW at flutter conditions as a common test case. The primary purpose of this study is to evaluate the effect of angle of attack. To do so, we analyzed BSCW wing at three angles of attack - $\alpha = 0deg$, $\alpha = 1deg$ and $\alpha = 5deg$. The second task is to evaluate the effect of gas composition on flutter boundary. The two gases are R-12 heavy gas, used as a test medium for the wind tunnel test, and air.

NOMENCLATURE

$BSCW$	Benchmark Super Critical Wing
CFD	Computational Fluid Dynamics
CSM	Computational Structural Mechanics
FRF	Frequency Response Function
LCO	Limit Cycle Oscillations
M	Mach number
q	dynamic pressure
ξ	damping ratio

1 INTRODUCTION

THIS paper is a contribution to the Aeroelastic Prediction Worskhop II [1–3]. The presented paper follows the paper of Jirasek et al. [4] which focused on assessment of the fluid-structure coupling scheme and its influence on the accuracy of transonic flutter prediction. The test case used in the paper [4] was a Benchmark Supercritical Wing, BSCW, at angle of attack 0 degrees.

This paper extends the investigation to higher angles of attack - $\alpha = 1$ degree and $\alpha = 5$ degrees - in order to asses its effect on the flutter boundary. The influence of angle of attack on the flutter

and limit cycle oscillations was studied by Tang et al. [5] and Attar et al. [6] who theoretically and experimentally investigated aeroelastic behavior on the delta wing in subsonic flow regime. It was shown that flutter speed depends non-linearly on the angle of attack. The first increase of the angle of attack led to increase of the flutter speed, further increase of the angle of attack caused decrease of the flutter speed. Yates et al. [7] focused on flutter behavior of the supercritical wing and shown the indirect proportional dependency of the flutter speed on the increased angle of attack.

The need of reaching realistic Reynolds numbers while keeping the model size to fit the size of available wind tunnel space, led to idea of using low temperatures and heavy gases as a test medium [8–10]. Apart from changing the value of Reynolds number the effect of gas composition on aeroelastic coefficients is not considered [8]. Rare studies of effect of gas on aeroelastic features of a tested object are available, they are however focusing on aeroelasticity in hypersonic flows where the primary motivation of using different than ideal gas is given by large differences in predicting correct effect of temperature rather then aeroelasticity [11, 12].

In this paper we try to evaluate effect of angle of attack and gas composition on flutter boundary of the BSCW wing at subsonic and transonic Mach numbers and Reynolds numbers identical to those of the NASA Langley TDT wing facility. In addition, for air we evaluate the effect of different Reynolds number.

2 COUPLED CFD-CSM SOLVER

2.1 CFD code Edge

The CFD flow solver used in this study is Edge [13], a finite volume Navier-Stokes solver for unstructured meshes. The Edge uses the central second order accurate scheme in space. The time integration uses fourth order Runge-Kutta scheme. It employs local-time-stepping, local low-speed preconditioning, multigrid and dual-time-stepping for steady-state and time-dependent problems.

For unsteady case, the employed numerical scheme is a dual-time-stepping scheme [14] of the second order accuracy in time. The convergence within each time step is controlled by setting a number of minimum subiterations or by the level of residual reduction. In our case we specified a fixed number of subiterations which was set to get a minimal reduction of the residuals below certain value, usually 2.5 orders of magnitude.

2.2 Structural solver

The structural solver uses a differential linear equations valid for a dynamic system with small displacements

$$M\ddot{x} + C\dot{x} + Kx = f \tag{1}$$

where x is the vector of structural coordinates, and $f(t)$ is the corresponding vector of forces. The M , C, and K are the mass, damping and stiffness matrices. The equation of motion is reduced to the form,

$$a_k\ddot{q}_k + 2\zeta_k a_k \omega_k \dot{q}_k + a_k \omega_k^2 q_k = Q_k, \qquad k \in [1, N_m] \tag{2}$$

where ζ is the *damping ratio* for mode k and

$$Q_k = \psi_k^T f \tag{3}$$

is the corresponding generalized force. The structural damping matrix, C, is a linear combination of the mass and stiffness matrices M and K, i.e. it is considered as a proportional or Rayleigh damping. As all cases considered in this case are at or close to flutter condition the damping was set to $C = 0$.

2.3 Coupling Scheme

The CFD-CSM coupling scheme which is used in this work is a partitioned coupling scheme in which both solvers are running separately, exchanging data on the common boundary which in this case is the surface of the wing. The data exchange includes sending the values of modal force coefficients from the CFD solver to CSM solver and sending modal coordinates from the CSM solver to the CFD solver.

The test case has just two modes (pitch and plunge), thus the computational mesh does not need to be deformed. Modal coordinates defines the wing vertical displacement and rotation around the y axis. So, the mesh is considered rigid and is rotated and translated as specified by the modal coordinates. This reduces the overhead due to mesh deformation to a minimum and allows to perform the CFD-CSM data exchange at every sub-iteration level, thus the scheme is a strong coupling scheme, [4].

3 TEST CASE

3.1 Experimental Setup

The test case is the Benchmark Super Critical Wing, BSCW, which was tested at NASA TDT facility [15]. This test case was chosen as one of the cases used in the Aeroelastic Prediction Workshop I and II [1–3]. The test data include measurements for the rigid, forced oscillations and aeroelastic problem. Since the wing itself is rigid, the elastic behavior in aeroelastic tests is allowed by using the Pitch and Plunge Apparatus, PAPA which allows simultaneous plunge and pitch of the wing [15]. Figure 1 shows the BSCW wing in NASA TDT wind tunnel section.

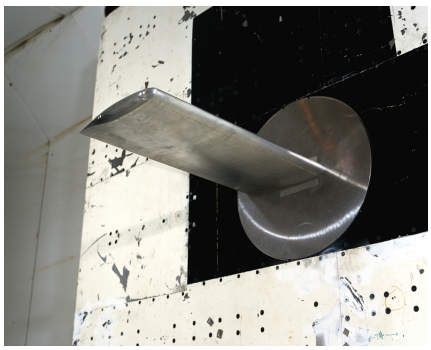

Figure 1: BSCW wing at NASA TDT wind tunnel section, Courtesy of NASA

The test case considered in this work is a case of flow around the BSCW at angle of incidence $\alpha = 0$ degrees. The flow at the angle of attack $\alpha = 0$ degrees is fully attached. The test medium is R-12 coolant gas.

3.2 Computational setup

The linear structural model has two modes - the plunging mode with frequency $f = 3.3Hz$ and pitching mode with frequency $f = 5.2Hz$ [3]. The pivotal point location is at 50% of the airfoil

chord (see Figure 2).

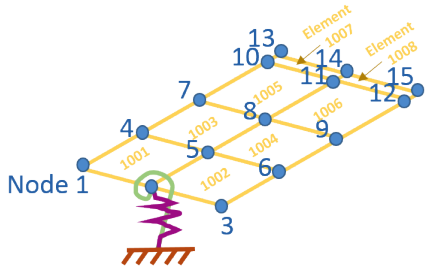

(a) Finite element model diagram

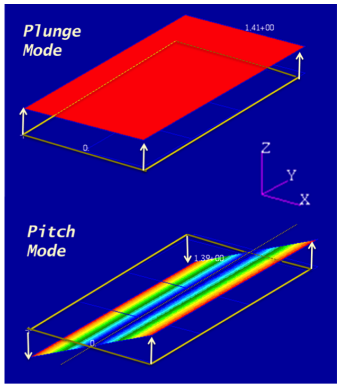

(b) Finite element model modes diagram

Figure 2: Finite element model [3]

The CFD mesh consist of 13 million points and is composed of tetra, prism and penta elements. The mesh is made according to the mesh guide specifications from the Aeroelastic Prediction Workshop I which is essentially copy of the mesh guide specification from the AIAA Drag Prediction Workshops. The guide specified details such as the thickness of the first prism layer on the wall, the number of cells across the trailing edge. The current mesh is a medium type of mesh shown in Figure 3.

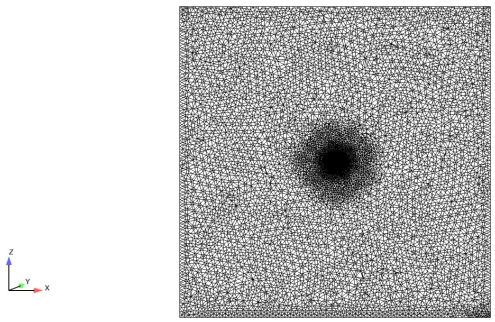

(a) Computational mesh

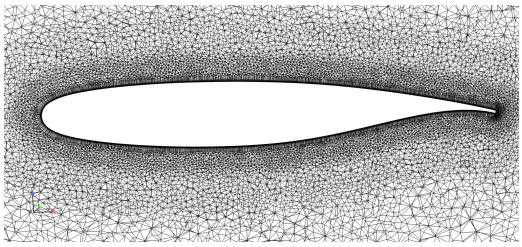

(b) Detail of the mesh around wing

Figure 3: Computational Mesh

The analysis is run in the unsteady, URANS mode using the Spalart Allmaras, SA model [16]. Each solution starts with a steady RANS analysis which is then used as an initial guess for URANS analysis of a steady wing. The well converged URANS solution around a steady wing is used as an initial guess for URANS coupled aeroelastic analysis which is run until it models between 3 to 5 seconds of the physical time. For some cases, especially those in range of Mach number $M = 0.8$ and higher, the sampling time was longer, up to 10 seconds.

4 RESULTS

The influence of two things on the flutter boundary is studied - effect of the angle of attack and effect of gas composition. Detailed investigation of gas effect was performed for the flutter point at Mach number $M = 0.74$ and results were compared with experimental data available for this condition.

4.1 Estimate of the flutter boundary - effect of angle of attack

The gas used for the analysis in this case is the R-12 coolant gas. The experimental data are available for angle of attack $\alpha = 0$ degrees, only. The wing was computationally analyzed at three angles of attack - 0 degrees, 1 degree and 5 degrees. For the angles of 0 and 1 degree it is reasonable to expect that the flow is fully attached at all Mach numbers, at angle of 5 degrees the flow is separated at higher Mach numbers (from M = 0.83 above).

The range of tested Mach numbers is from 0.6 to 0.9. Comparing the cases of 0 and 1 degree (Figure 4(a)), the only difference occurs at high Mach number $M = 0.9$. In the case of higher angle of attack, the shock wave reaches the trailing edge at slightly lower Mach number than for case of $\alpha = 0degress$ reaching the region of Mach number freeze earlier.

For wing at angle of attack $\alpha = 5$degrees the values of dynamic pressures are lower then for lower angles of attack at entire range of tested Mach numbers. A flutter dip is noticeable at Mach numbers around $M = 0.8$ and at Mach number $M = 0.83$ the results indicates the presence of the limit cycle oscillation, LCO at dynamic pressures lower than $q = 4000$Pa. In the case of $\alpha = 5degs$ and $M = 0.9$ the flutter point is not shown because at these conditions the wing is stable for all investigated dynamic pressures up to $q = 15000$Pa (the damping coefficient increases proportionally with the dynamic pressure).

The plot of flutter frequency presented in Figure 4(b) shows that in cases of low angles of attack the frequencies are comparable in whole range of analyzed Mach numbers. In the case of angle of attack $\alpha = 5$degrees, there is evident increase of flutter frequency in range above Mach number $M = 0.7$.

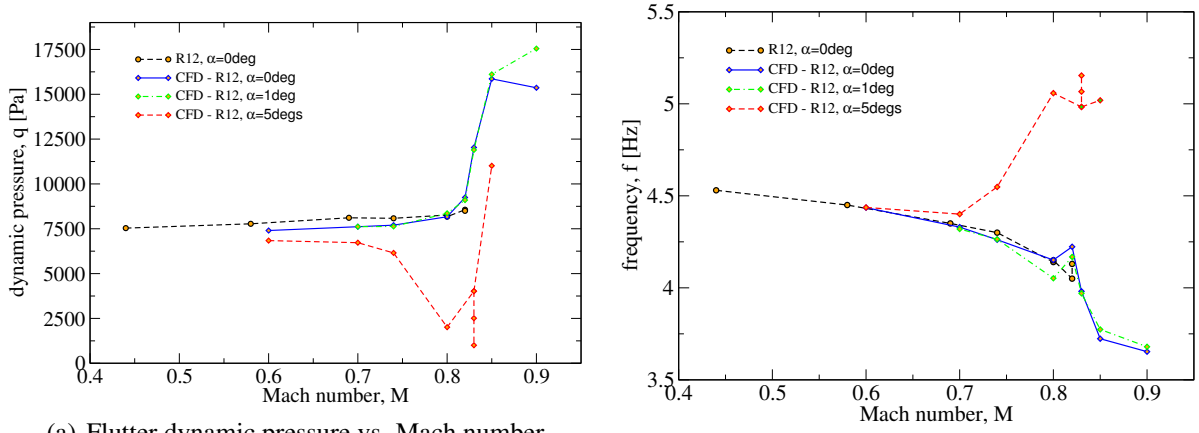

(a) Flutter dynamic pressure vs. Mach number

(b) Flutter frequency vs. Mach number

Figure 4: Flutter curve for wing at different angles of attack

The Figure 5(a) shows the value of damping coefficient versus dynamic pressure at Mach number $M = 0.83$, $\alpha = 5$ degrees. For the range of dynamic pressures up to $q = 4000Pa$, the values of damping coefficient are located around $\xi = 0$ suggesting all points within this range are points of the neutral damping. At higher dynamic pressures the motion is then divergent and wing is in flutter. Figure 5(b) shows the pitching motion amplitude vs dynamic pressure, the curve is almost linear for dynamic pressures where wing is at LCO.

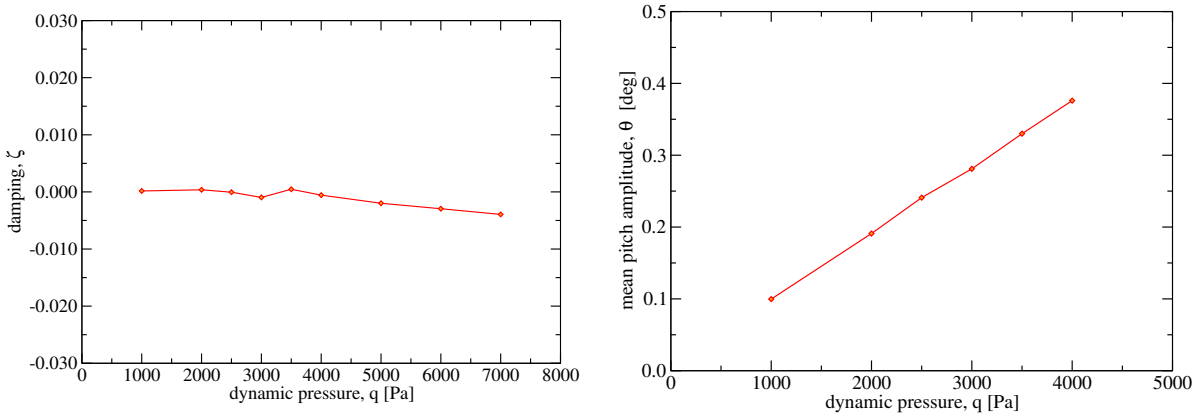

(a) Damping coefficient

(b) Pitch mode amplitude

Figure 5: Damping coefficient and pitching motion amplitude vs. dynamic pressure at $M = 0.83$ and $\alpha = 5$ deg

4.2 Estimate of the flutter boundary - effect of Reynolds number and gas composition

Two gases were used for the estimation of the gas effect on the flutter boundary - the R-12 gas and the air. The wind tunnel measurement data are available for these gases and the wing angle of attack $\alpha = 0$ degrees.

The analysis using air was done for two flow conditions. The first case uses the same free-stream temperature as the R-12 gas tests. This setup results in lower Reynolds number due to effect of different viscosity and gas constant of the air (see Figure 6). In the other case, the free-steam temperature was adjusted in order to obtain the same Reynolds number at each Mach number as for the R-12 case gas. So the comparison in Fig 6 shows the effect of gas and effect of Reynolds number for air.

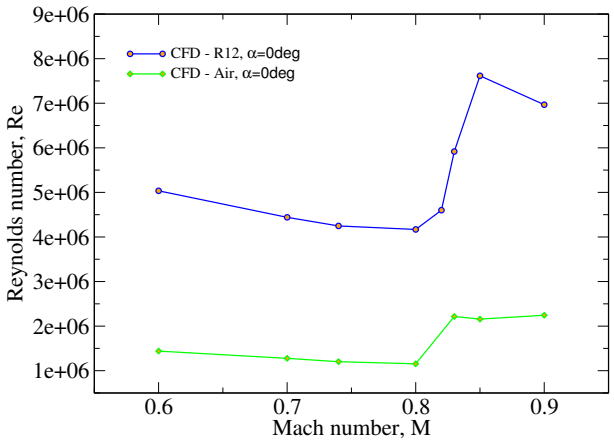

Figure 6: Comparison of Reynolds numbers at flutter points in different Mach numbers - R-12 gas and air at the R-12 temperature

The comparisons show strong effect of both gas composition and Reynolds number. At lower Mach numbers where the flow is subsonic, the effect of gas composition is very small, as indicated both by CFD runs and wind tunnel test. The effect of Reynolds number contributes to lower values of the dynamic pressure as the Reynolds number gets lower. At $M = 0.8$ and higher the effect of Reynolds number is almost smaller then effect of gas composition. Interestingly the air at higher Reynolds number shows an indication of small transonic dip at Mach number around $M = 0.8$ which is not present for R-12 gas and air at lower Reynolds number. At $M = 0.85$ the results of air at Reynolds number of R-12 gas get closer to R-12 gas indicating

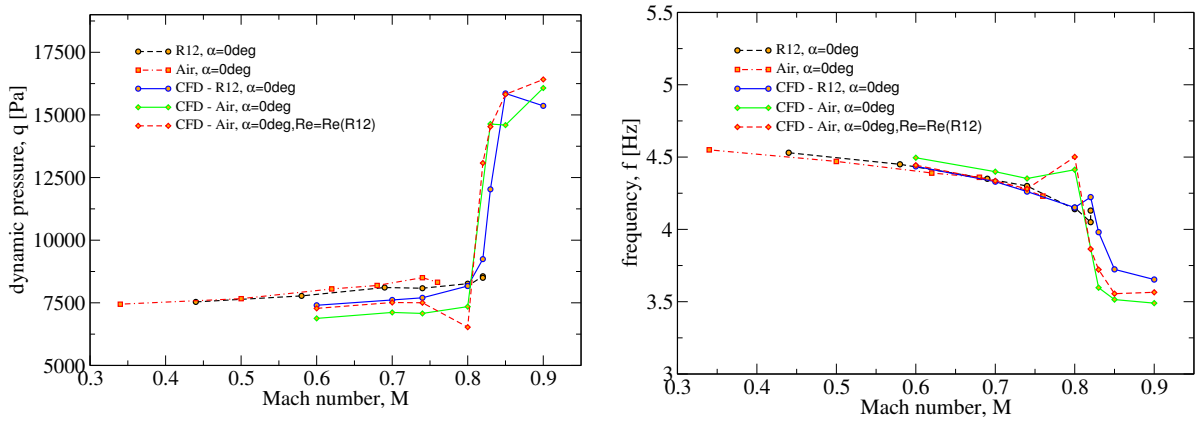

(a) Flutter dynamic pressure vs. Mach number

(b) Flutter frequency vs. Mach number

Figure 7: Flutter curve for different gases

that the Reynolds number effect is getting more important then gas composition. In general, the result clearly show that in the area of transonic flow with shock wave boundary layer interaction, which has a very strong effect on flutter dynamic pressure, the effect of gas and Reynolds number are both important. In other areas, either at subsonic Mach numbers or higher transonic Mach numbers, where the wing is approaching Mach number freeze, the effect of Reynolds number is the dominant effect.

4.3 Investigation of flutter point at M = 0.74 - effect of Reynolds number and gas composition

Figures 8 and 9 show magnitude and phase of pressure coefficient frequency response function (FRF) at 60% and 95% of span. Experimental data are compared with computationally obtained flutter points of cases using R-12 gas and air at both conditions at Mach number $M = 0.74$ and $\alpha = 0$ degrees.

The comparison of FRF show slight difference in the phase at 60% span cut which is probably due to both gas and Reynolds number effect on dynamic behavior of the post-shock flow separation. At 95% wing span, the effect of Reynolds number is rather large and is concentrated around the shocks. It is probably the results of different shock structure due to lower Reynolds number as well as different dynamic behavior of the post-shock flow separation. It should be noticed the abrupt jumps of the phases are 360 degrees phase shifts, only.

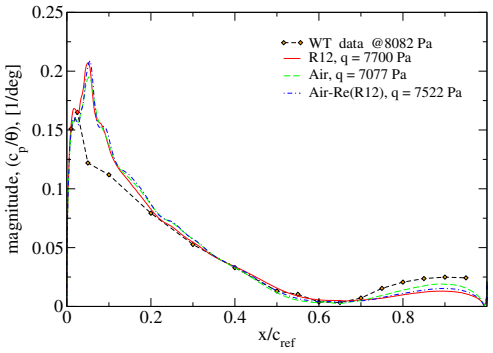

(a) Magnitude lower side - 60%

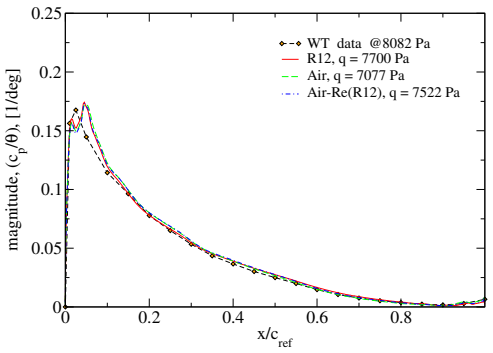

(b) Magnitude upper side - 60%

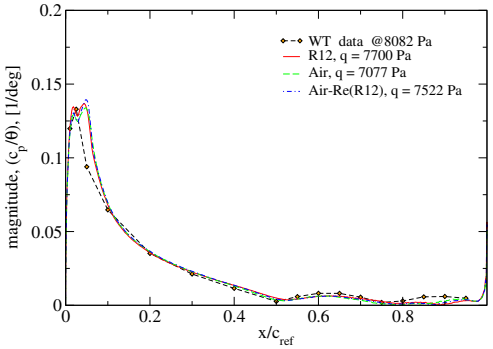

(c) Magnitude lower side - 95%

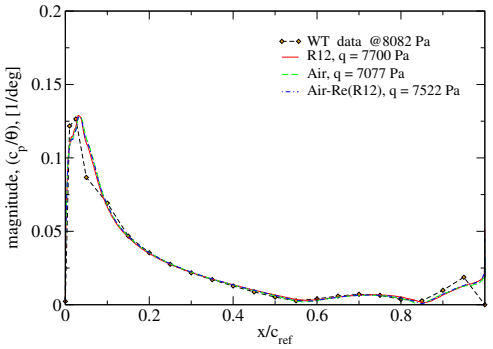

(d) Magnitude upper side - 95%

Figure 8: Magnitude in 60% and 95%

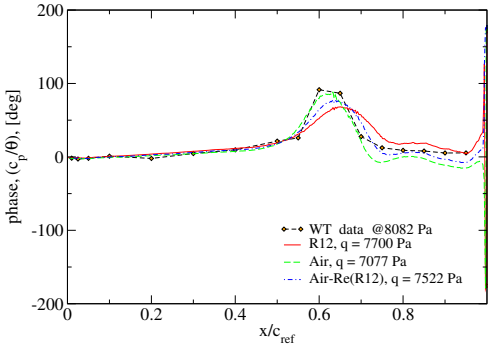

(a) Phase lower side - 60%

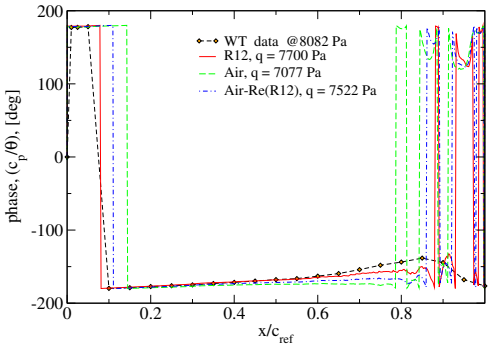

(b) Phase upper side - 60%

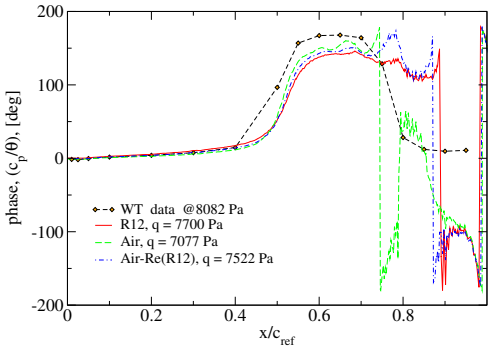

(c) Phase lower side - 95%

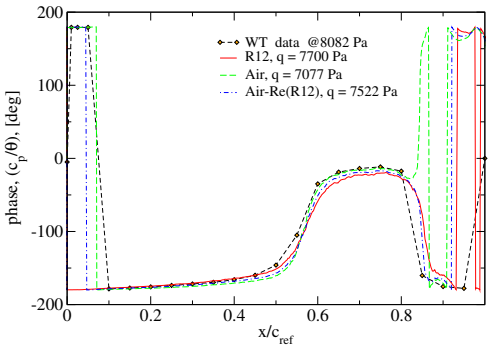

(d) Phase upper side - 95%

Figure 9: Phase in 60% and 95%

5 CONCLUSION

This paper presents study of the Benchmark supercritical wing at flutter conditions. The first part focuses on assessing the effect of angle of attack on flutter boundary. Comparing the cases of lower angles of attack $\alpha = 0$ and 1 degree at lower Mach numbers the flutter boundary is marginally effected by angles of attack. The only visible effect occur at high Mach number where the wing at higher angle of attack reaches the area of Mach number freeze earlier.

For high angle of attack of $\alpha = 5$ degrees the flutter dynamic pressures are generally lower. The flutter curve shows earlier onset to non-linear aeroelasticity and the flutter curve shows the presence of the flutter dip at Mach number between $M = 0.8$ and $M = 0.83$. The limit cycle oscillations are present at $M = 0.83$ at dynamic pressures below $q = 4000Pa$. At higher Mach numbers around $M = 0.9$ the wing at higher angle of attack reaches the area of Mach number freeze earlier compared to wing at lower angles of attack.

The second part focuses on evaluation of the effect of the gas composition and Reynolds number on the flutter curve. It shows that effect of gas composition is mostly important in the region of transonic Mach numbers where there is a strong effect of shock wave boundary layer iteration. For other Mach numbers the effect of gas composition is mild or marginal. The effect of Reynolds number is present in almost entire range of tested Mach numbers even at low subsonic Mach numbers. This is very possibly due to effect of Reynolds number on the dynamics of the flow separation for both subsonic and transonic Mach numbers. The conclusion of this section is that modeling of correct Reynolds number is more important than the effect of gas composition.

ACKNOWLEDGMENTS

The research received funding from the Ministry of Education, Youth and Sports of the Czech Republic under the National Sustainability Programme I - Project LO1202.

This work was supported by The Ministry of Education, Youth and Sports from the Large Infrastructures for Research, Experimental Development and Innovations project „IT4Innovations National Supercomputing Center LM2015070".

Authors would like to acknowledge the support of High Performance Modeling and Simulation Center at the United States Air Force Academy.

Authors would like to thank Jennifer Heeg and Pawel Chwalowski of NASA for providing data, post-processing scripts and numerous consultations.

6 REFERENCES

[1] Heeg, J., Chwalowski, P., Florance, J. P., et al. Overview of the aeroelastic prediction workshop. AIAA 2013-783, 51st AIAA Aerospace Sciences Meeting including the New Horizons Forum and Aerospace Exposition. January, 2013.

[2] Heeg, J., Chwalowski, P., Schuster, D. M., et al. Plans and example results for the 2nd aiaa aeroelastic prediction workshop. AIAA 2015-0437, 56th AIAA/ASCE/AHS/ASC Structures, Structural Dynamics, and Materials Conference. January.

[3] Aeroelastic prediction workshop 2. http://nescacademy.nasa.gov/workshops/aepw2/public/.

[4] Jirásek, A., Dalenbring, M., and Navrátil, J. (2016). Computational fluid dynamics study of benchmark supercritical wing at flutter condition. *AIAA Journal*.

[5] Tang, D. and Dowell, E. H. (2001). Effects of angle of attack on nonlinear flutter of a delta wing. *AIAA journal*, 39(1), 15–21.

[6] Attar, P., Dowell, E., and Tang, D. (2003). A theoretical and experimental investigation of the effects of a steady angle of attack on the nonlinear flutter of a delta wing plate model. *Journal of Fluids and Structures*, 17(2), 243–259.

[7] Yates Jr, E. C. and Chu, L.-C. (1987). Static aeroelastic effects on the flutter of a supercritical wing.

[8] Hanson, P. W. (1980). An assessment of the future roles of the national transonic facility and the langley transonic dynamics tunnel in aeroelastic and unsteady aerodynamic testing. Tech. rep.

[9] Kilgore, R. A., Igoe, W. B., Adcock, J. B., et al. (1979). Full-scale aircraft simulation with cryogenic tunnels and status of the national transonic facility.

[10] Howell, R. R. and McKinney, L. W. (1976). The us 2.5-meter cryogenic high reynolds number tunnel.

[11] Lamorte, N. and Friedmann, P. P. (2014). Hypersonic aeroelastic and aerothermoelastic studies using computational fluid dynamics. *AIAA Journal*, 52(9), 2062–2078.

[12] McNamara, J. and Friedmann, P. (2007). Aeroelastic and aerothermoelastic analysis of hypersonic vehicles: Current status and future trends. In *48th AIAA/ASME/ASCE/AHS/ASC Structures, Structural Dynamics, and Materials Conference*. p. 2013.

[13] Eliasson, P. (2002). EDGE, a Navier-Stokes solver for unstructured grids. In *Proc. to Finite Volumes for Complex Applications III*. ISBN 1 9039 9634 1, pp. 527–534.

[14] Jameson, A. Time dependent calculations using multigrid, with application to unsteady flows past airfoils and wings. AIAA 91-1596, AIAA 10th Computational Fluid Dynamics Conference, June 24-26, 1991, Honolulu HI, USA.

[15] Heeg, J. and Piatak, D. J. Experimental data from the benchmark supercritical wing wind tunnel test on an oscillating turntable. AIAA Paper 2013-1802, 54th AIAA/ASME/ASCE/AHS/ASC Structures, Structural Dynamics, and Materials Conference, 8-11 Apr 2013; Boston, MA, United States.

[16] Spalart, P. R. and Allmaras, S. R. (1994). A one-equation turbulence model for aerodynamic flows. *Recherche Aerospatiale*, 1, 5–21.

COPYRIGHT STATEMENT